Visual and Electrical Evidence Supporting a Two-Plasma Mechanism of Vacuum Breakdown Initiation

Carlos H. Castano, Maro Aghazarian, John B. O. Caughman, II, and David N. Ruzic

***Abstract*—The energy available during vacuum breakdown between copper electrodes at high vacuum was limited using resistors in series with the vacuum gap and arresting diodes. Surviving features observed with SEM in postmortem samples were tentatively correlated with electrical signals captured during breakdown using a Rogowski coil and a high-voltage probe. The visual and electrical evidence is consistent with the qualitative model of vacuum breakdown by unipolar arc formation by Schwirzke [1, 2]. The evidence paints a picture of two plasmas of different composition and scale being created during vacuum breakdown: an initial plasma made of degassed material from the metal surface, ignites a plasma made up of the electrode material.**

***Index Terms*—Breakdown model, plasma material interactions, unipolar arc, vacuum breakdown.**

I. Introduction

VACUUM BREAKDOWN has been studied for more than a century [3], and some of the details are still not understood [4], [5]. Part of the reason is that at the moment of a breakdown, the four states of matter coexist for a very short period of time in a microscopic volume of space with catastrophic destruction of the location. It is challenging to devise diagnostics that provide in situ information and the analysis and interpretation of the postmortem breakdown sites are far from trivial [6]. A better engineering understanding of the preliminary steps causing breakdown can help prevent unintended breakdown and usher a new era of vacuum engineering applications with significantly improved vacuum dielectric strength. Vacuum breakdown is of great technological importance in a variety of applications including space propulsion [7], direct nuclear to electrical energy conversion [8], high power RF antennas [9], [10], particle accelerators [11], novel X-ray sources [12], and many others.

Manuscript received August 26, 2011; revised December 4, 2011; accepted January 4, 2012. Date of publication March 19, 2012; date of current version April 11, 2012. This project was funded at the University of Illinois by the U.S. Department of Energy with Grant DE-FG02-04ER54765 (contract monitored by T. V. George), and supported by Oak Ridge National Laboratory, managed by UT-Battelle, LLC, for the U.S. Department of Energy under contract DE-AC05-00OR22725. SEM images were obtained in the Center for Microanalysis of Materials, University of Illinois, which is partially supported by the U.S. Department of Energy under Grant DEFG02-91-ER45439.

C. H. Castano is with the Nuclear Engineering, Missouri University of Science and Technology, Rolla, MO 65409 USA (e-mail: castanoc@mst.edu).

M. Aghazarian and D. N. Ruzic are with the Center for Plasma Material Interactions, University of Illinois, Urbana, IL 61801 USA (e-mail: marojan@gmail.com; druzic@illinois.edu).

J. B. O. Caughman is with the Fusion Energy Division, Oak Ridge National Laboratory, Oak Ridge, TN 37830 USA (e-mail: caughmanjb@ornl.gov).

Digital Object Identifier 10.1109/TPS.2012.2186466

It has been suggested that vacuum breakdown occurs by way of unipolar arc formation with a clear sequence of stages [1], [2], [13]. We present here evidence that on high vacuum (10^{-8}–10^{-6} Torr) breakdown proceeds in two separate phases. The first stage includes the formation of a relatively large plasma ($\sim$100 μm diameter) arguably formed from gas molecules degassed from the surface and ionized by field emitted electrons. The second stage initiates at a localized spot ($\sim$few μm diameter) and corresponds to plasma of vaporized electrode material (metal). This second stage is mostly responsible for the destruction of the electrode in uncontrolled vacuum arcs. While there are other more mathematically intensive 3-D models of vacuum breakdown [14], as well as quantitative analysis of assumed nonequilibrium plasma conditions during breakdown [15], the 1-D Schwirzke model is simple and elegant enough to illustrate and explain the experimental results presented here. More detailed models, which have to assume multiple conditions, should wait until better diagnostics are available to study microscopic plasmas in situ with enough time resolution during breakdown events.

II. Experimental Procedure

The experimental setup consist of two copper (99.999%) parallel plate electrodes with polished Rogowski profiles [16] inside a vacuum chamber evacuated using a turbomolecular pump. The chamber achieved ultimate pressures down to 4.1×10^{-8} Torr measured with a glass Alpert-Ballard ionization gauge.

The high voltage is provided by a 50-kV capacitor-charging power supply General Atomics CCS (previously Maxwell Labs) model CCS-08-050-P-1-0000-C. This power supply requires a capacitive load present at all times to work properly which is provided by a 52 μF capacitor. Polarity inversion prevention during breakdown experiments is required for the power supply and is provided by a diode network of 22 $-$ 1 kV diodes, varistors, and resistors (see Fig. 1) connected to the output of the power supply. In series with the vacuum gap, there is a current limiting resistor (R_{series}), which can be changed as needed for each experiment. The emission current is measured using a 1 kΩ thick-film noninductive precision resistor on the ground side of the gap (R_{shunt}) as shown in Fig. 1, allowing reproducible measurements down to 1 nA currents. R_{shunt} is redundantly protected from overcurrent by a Zener diode, a varistor, and three neon NE-2 lights connected

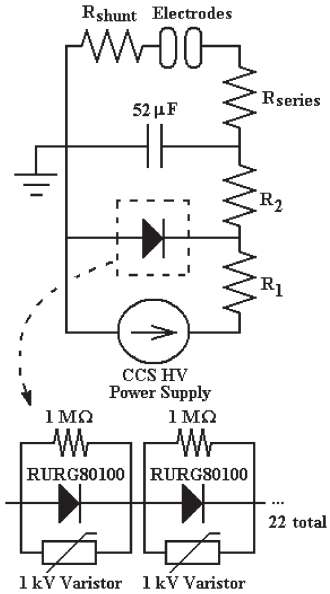

Fig. 1. High voltage breakdown experimental setup. R_{series} limits energy going to the arc. R_{shunt} (noninductive, 1 kΩ) is used to measure emission current. $R_1 = R_2$ (225 Ω, 150 W) provide current limitation and load balance for the CCS HV power supply. 22-kV Polarity inversion protection for the CCS HV power supply is provided by the diode assembly consisting of 22 RURG80100 (80-A, 1000-V Ultrafast Diodes), 1 MΩ resistors and 1-kV Varistors.

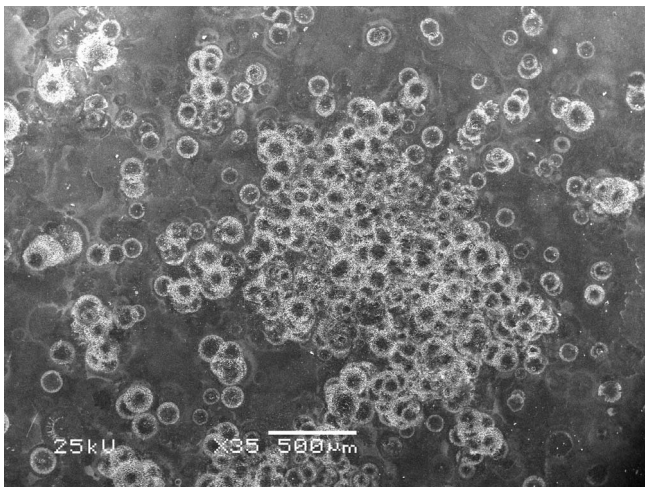

Fig. 2. Breakdown marks on the cathode of parallel copper electrodes obtained by limiting the current going into the arc with a 1 MΩ resistor in series. $Vb = 5$–20 kV.

in parallel. R_{shunt} can be short-circuited and R_{series} bypassed to perform high current experiments, or plasma conditioning of the electrodes using the same power supply.

The gap between the electrodes is measured and controlled using a linear motion feedthrough with a stroke of 5.08 cm ($2''$) and reproducible gap control of ± 1 μm in the horizontal direction. During long horizontal displacements, we found that the feedthrough wobbles. Wobbling is as much as 1 mm in the vertical direction for 1 cm of horizontal displacement. Nonetheless, its performance is adequate in the scale of our experiments (gap changes smaller than 100 μm) since at that scale the electrode faces remain parallel.

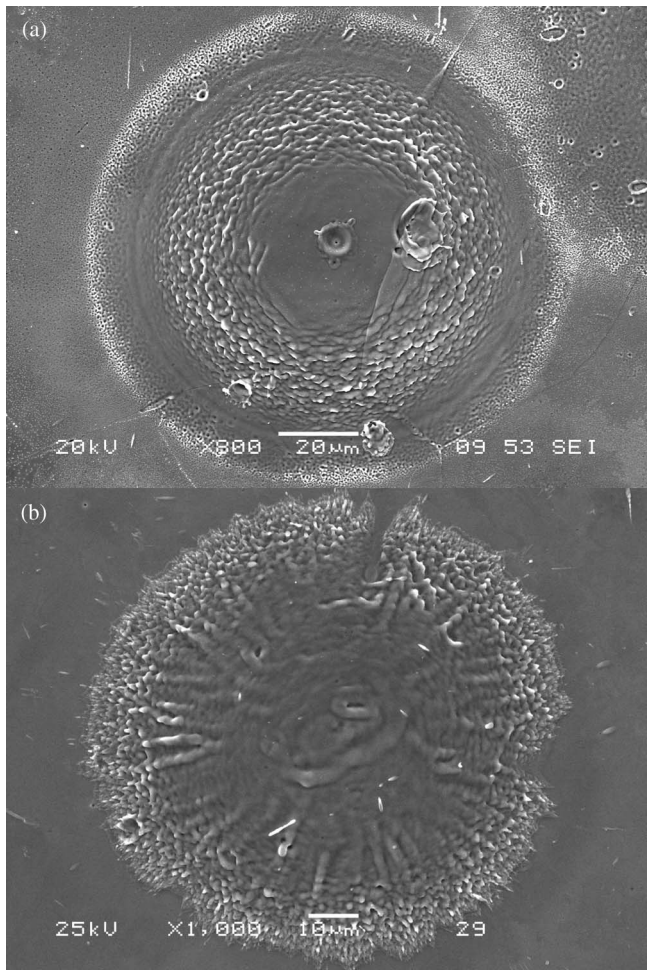

Fig. 3. Typical breakdown marks (a) with and (b) without central crater. Breakdown events with current limited by $R_{\text{series}} = 1$ MΩ($R_{\text{shunt}} = 1$ kΩ).

The voltage of the high-voltage electrode is recorded using a PHV 4002-3 0.6 ppm/V 1000X High Voltage Probe in the range of 2–20 kV DC (minimum accuracy $= 0.083\%$). The output of the probe is matched to a 1 MΩ impedance. Capture of breakdown events is performed using both a Lecroy 9304A Quad 200 MHz 100 MS/s Digital Storage Oscilloscope with a computer interface, and a Tektronix TDS 2014 100 MHz 1 GS/s digital oscilloscope.

The breakdown current was measured using a series resistor (R_{shunt}) for small emission current (1 nA-mA's), and a Rogowski coil current transducer for large breakdown currents (few to 100's of Amps). Using an unprotected series resistor poses some risk to the oscilloscope, since at the moment of a breakdown, the current is unpredictable and the signal is not DC (it consists of several MHz pulses lasting a few μs followed by a ms pulse of lower frequency). Careful design of the Rogowski current transducer coil was required [17], [18], including consideration of the frequency of the measured signal [19] to protect it. Details of the equation derivation and behavior of the different types of integrators can be seen elsewhere [20].

III. Results

Using a limiting resistor (R_{series}) of 1 MΩ allowed the isolation of separate incidents of breakdown so that multiple

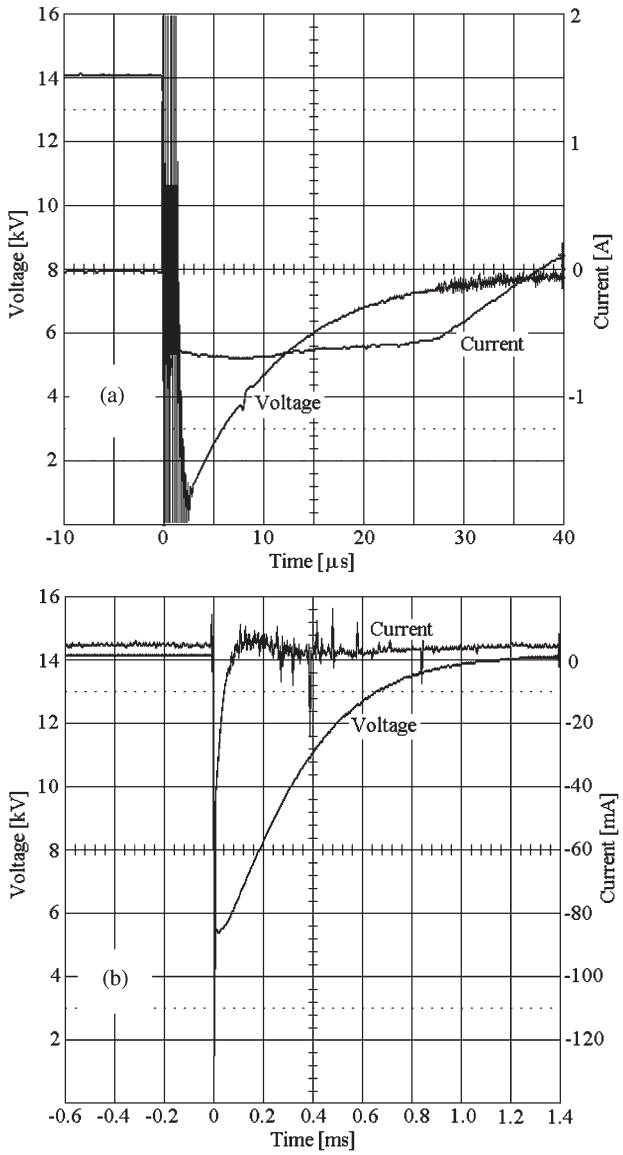

Fig. 4. Oscilloscope traces illustrating the timescale of the current signal during two typical 14-kV breakdown experiments ($R_{\text{series}} = 1$ MΩ, $R_{\text{shunt}} = 10$ Ω). Notice the short (∼2–3 μs) intense oscillatory current in (a), followed by a longer lived low frequency component (∼100 μs) more clearly seen in a millisecond scale in (b).

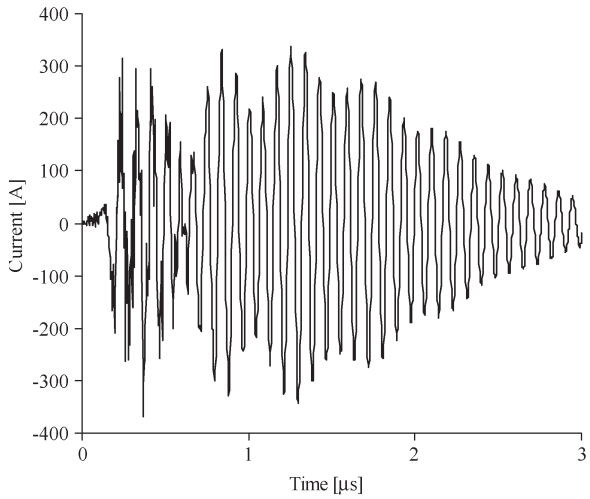

Fig. 5. Rogowski coil measurements of currents of hundreds of amperes during the initial 3 μs of an isolated breakdown event ($R_{\text{series}} = 1$ MΩ, $R_{\text{shunt}} \cong 0$).

breakdowns can occur at slightly different places without complete destruction of the breakdown spot. The breakdowns occur in different places as expected from theory since arc initiation destroys the micro-emitter that originates them [10]. Typical breakdown marks are shown in Fig. 2. While these marks come in different sizes (48–238 μm), some present a crater-like central feature [see Fig. 3(a)], and some do not [see Fig. 3(b)]. We think that this difference can be related to difference in the electrical signals detected during the breakdown events. The current detected during individual arcs is variable, and this likely accounts for the different size of the observed features. The outward pointing features in the rims of Fig. 3(a) and (b) are likely formed by electric field stretching of molten metal in contact with a plasma [5]. Further analysis of those patterns is presented in the discussion section.

Two oscilloscope traces of breakdown events captured by a Lecroy 9304A oscilloscope are shown in Fig. 4. Due to the parallel plate electrode configuration and the small gap, the exact position of each breakdown was not possible to determine with parallel electrodes, such that a definitative correlation between breakdown images with electrical signals was not possible. Nevertheless, both the photographic features and the oscilloscope traces were consistently obtained over many experiments. We used these typical results to explain the features observed. An experimental effort, presented elsewhere [20], was conducted to correlate individual breakdown events with features in sharp tips prepared by electropolishing, and it supports our current correlation.

The oscilloscope traces in Fig. 4 show a breakdown event split in two main parts. An initial intense current pulse lasting ∼2–3 μs, followed by a longer lived current component of less than 100 μs which accounts for currents between 40 and 775 mA (measured with the series resistor). To determine the current of the initial 2–3 μs component, a Rogowski transducer coil method was used indicating currents on the order of 100's of Amps (RMS ∼ 114.6 A, see Fig. 5). The Rogowski coil was calibrated using signals from 0.25 to 14 A, and a linear behavior through seven points $(R = 0.9994)$ was obtained (Rogowski coils are well known to tolerate extrapolation because their behavior is highly linear [19]). Because the insulator used to wind the Rogowski coil (rubber silicone) has an unknown dielectric constant, the cutoff frequency for linear behavior is only estimated. To make sure we were observing a real signal and not a resonance on the coil above the cutoff frequency, another Rogowski coil with different size and electrical parameters was employed. The cutoff frequency of the second coil was estimated to be 400% higher than the original coil, yet the frequency of the signal detected was only 3% different, thus we concluded that our measurement were indeed correct, and the coil was operating within the frequency range that exhibit constant gain [19].

One final important observation in our experiments is that a breakdown event will sometimes not produce the long-lived

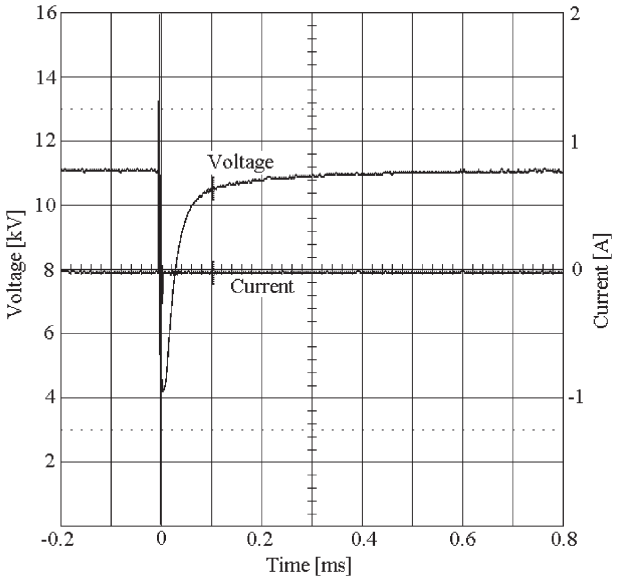

Fig. 6. Breakdown event in which only the initial short current pulse (2–3 μs) is present, without a long-lived current component. The voltage drop is the clear indication of a breakdown occurrence.

current component, such that only the initial short ($\sim \mu$s) current pulse is present. The lack of current long-lived component shown in Fig. 6 suggests a difference in different breakdown events. We propose that these signals correspond to breakdown marks such as those shown in Fig. 3(b) without the central crater as explained in the next section.

IV. Discussion

A. Schwirzke Model

We interpret Figs. 3–6 in light of the Schwirzke unipolar arc qualitative model [1]. Schwirzke's model has also been used successfully to explain or correlate data from breakdown in other applications [21]–[26]. The diameter of features and the currents measured correlate well according to this model. The stretched molten metal features pointing outwards in the circular external rims of Fig. 3(a) and (b) suggest the presence of a plasma, which is not surprising since during breakdown events arcs are observed and expected. Such features are explained by electric-field stretching of molten metal in contact with a plasma [6].

Following Schwirzke's qualitative model (which will suffice to explain the experiment), the electric field (E_s) due to the plasma sheath can be approximated by the plasma floating potential (V_f) divided by the Debye length (λ_D). V_f of a metal in contact with a plasma, can be calculated from the electric field needed to balance the ion and electron flux [27], as

$$V_f = \frac{kT_e}{2e} \ln\left(\frac{m_i}{2\pi m_e}\right) \tag{1}$$

where T_e is the electron temperature, k is the Boltzmann constant, e is the elementary charge, m_i, and m_e are the ion and electron mass, respectively. Dividing by the Debye length, we obtain

$$E_s = \frac{V_f}{\lambda_D} = \sqrt{\frac{n_e k T_e}{4\varepsilon_0}} \ln\left(\frac{m_i}{2\pi m_e}\right). \tag{2}$$

A n_o value is suggested in [2] by assuming that at the beginning of the process the surface suddenly releases about a monolayer's worth of gas, $\sim 2 \times 10^{15}$ molecules/cm^2, a figure supported in our experiments by the pressure change measured during a single breakdown event [28]. Schwirzke assumes that the gas released expands at the speed of sound ($\upsilon \approx 3.3 \times 10^4$ cm/s, pressure independent in an ideal gas) and reaches the zone of maximum ionization (100 eV) after 3 ns, the density of the gas in front of the emitter, where the plasma is formed would be $n_0 \approx 2 \times 10^{15}$ cm$^{-2}/\upsilon t \approx 2 \times 10^{19}$ cm^{-3} (614 Torr, but in a very small volume). Assuming conservatively that the ionization fraction is only $\sim 10^{-4}$, gives an estimated electron density, $n_\mathrm{e} = 2 \times 10^{21}$ m^{-3}.

Taken T_e to be 18 eV, a typical value of other plasmas known to produce unipolar arcing [29], (2) gives $E_\mathrm{s} = 3.5$ GV/m. This electric field combined with moderate heating of surface by ion bombardment ($> 0.3\, T_\mathrm{m}$) is sufficient to cause atom migration at the metal surface [30] arguably causing further electric field enhancement. Finally, since $E_\mathrm{s} \propto n_\mathrm{e}^{1/2}$, the plasma density is the main factor on enhancing the electric field.

In summary, the point where the plasma originated (due to local field enhancement) has now even more enhancement due to the presence of the plasma, causing higher currents that modify the emitter such that a very localized ($\sim \mu$m) hot metal vapor can be ionized and produce a second plasma. This second plasma is different from the original plasma in that it is made up of metal atoms (not degassed material). In the current research, this second plasma is the one that is quenched by limiting the current available through R_series. Otherwise, the current would be only limited by how much energy the power supply can provide, causing a continuous arc and massive damage to the electrode (ordinary arcs) and destroying in the process all features of interest relevant to the early stages of vacuum breakdown.

B. Correlation of Current and Features

The size of the features observed in Fig. 2 can then be explained as follows. The electron return current (i_s^-) from a unipolar arc is determined by the electron density (n_e) and the electron thermal velocity (υ_e), and is equal to [31]

$$i_s^- = \frac{1}{4} e n_e \upsilon_e A. \tag{3}$$

A is the area on the surface of the electrode where current is flowing. The measured current during the arcs can be used to estimate the area needed for the electron return current. These values should be consistent with the feature sizes shown in the arcs of our system in Fig. 3. The mean random thermal electron velocity (υ_e) is

$$\upsilon_e = \left(\frac{8kT_e}{\pi m_e}\right)^{1/2}. \tag{4}$$

From the current measurements shown in Fig. 4, there are two different currents and time scales in the arcs. In the first part, the current is oscillating with $\sim$11 MHz frequency in the order of several hundred amps and last only 2–3 μs. Taking the RMS value of the oscillating current which is 114.6 A, as the characteristic value and using the equation for i_s^-, the expected diameter for circular marks of the electrode would be 142 μm, which given the experimental setup and approximated model is in reasonable agreement with the overall size of the features presented in Figs. 2 (48–238 μm), and 3(a) and (b) ($\sim$88 and 97 μm, respectively).

The second stage of breakdown (second plasma) lasts $\sim$100 μs and exhibits much smaller currents ranging from 40 mA to 780 mA. For this current range, the expected feature diameter [using (3)] would be between 2.7 and 12.8 μm, which is in good agreement with the central feature present on Fig. 2(a) which is approximately 8 μm. The central hole $\sim$0.4 μm in size observed probably corresponds to the place where the emission current vaporized the original emitter whose nature is still unresolved, but clearly corresponds to a submicrometer feature (e.g., size grain boundary, impurity, oxide, or other insulator material located at the spot [4], [32]). These submicrometer holes are characteristic of unipolar arcs and have been observed in other studies [2].

Note that the initial plasma ($\sim$2–3 μs) is extinguished when it exhausts its source of ionizable material (gas desorbed form the surface). Assuming most of the gas is released during the ignition of the first plasma by the time the plasma reaches a size of a semisphere of $\sim$100 μm (size of typical marks of Fig. 2) the density is only 7.6×10^{19} m^{-3} $\approx$ 2 mTorr. Which is not enough pressure to sustain continuous ionization, and the plasma simply extinguishes without further damage to the electrode [Fig. 3(b)]. This phenomenon contributes to the principle of conditioning of electrodes. Conditioning seems to remove or modify the initial emitters, but also removes the source of ionization for the triggering plasma (stage 1). If the first plasma is arrested either way, full breakdown will not proceed as long as not enough energy is provided to the second plasma to ionize the metal atoms.

V. Conclusion

Individual breakdown initiation spots were isolated by limiting the energy available during breakdown events. This was possible because breakdown events destroy the emitter originating them, making subsequent breakdowns occur at slightly different locations. The preservation of breakdown spots allows postmortem studies of breakdown initiation sites.

Postmortem breakdown features observed on copper electrodes at high vacuum suggest breakdown initiation in two plasma stages. During the first stage oscillating currents up to several hundred amperes lasting only 2–3 μs were observed. The second stage exhibit currents of less than 1 A lasting 100's of microseconds. In some cases, the second stage was not observed.

The features observed with scanning electron microscopy can be explained by plasma material interaction between the electrode material and the two plasmas inferred. The stage one plasma is created from gasses released from the surface, followed by a second plasma formed from electrode material and ignited by the first plasma.

The correlation between breakdown currents measured and the size of the electrode marks (following Schwirzke's likely plasma parameters) suggests that vacuum breakdown at high vacuum proceed on two plasma stages. The initial intense current packet (2–3 μs, $I > 100$'s A) is responsible for the creation of the $\sim$100 μm outer rim in Fig. 3(a) and (b). While the central crater feature of Fig. 3(a) is produced by the longer-lived second current packet ($\sim$100 μs, $I < 1$ A). This second energy packet also marks the beginning of metal ionization, such that in cases where the current is not controlled it would cause the destruction of the metal electrode and a full-fledged arc.

The presence of breakdown marks without a crater-like central feature [Fig. 3(b)] corresponds to cases where the second plasma stage was not ignited. Never the less the stage one plasma destroys the original emitter "conditioning" the electrode such that breakdown is less likely.

References

[1] F. Schwirzke, "Onset of breakdown and formation of cathode spots," *IEEE Trans. Plasma Sci.*, vol. 21, no. 5, pp. 410–415, Oct. 1993.

[2] F. R. Schwirzke, "Vacuum breakdown on metal surfaces," *IEEE Trans. Plasma Sci.*, vol. 19, no. 5, pp. 690–696, Oct. 1991.

[3] R. W. Wood, "A new form of cathode discharge and the production of X-rays, together with some notes on diffraction," *Phys. Rev.*, vol. 5, no. 1, pp. 1–10, Jul. 1897.

[4] R. Latham, *High Voltage Vacuum Insulation, Basic Concepts and Technological Practice*. London, U.K.: Academic, 1995.

[5] A. Anders, *Cathodic Arcs, From Fractal Spots to Energetic Condensation*. New York: Springer-Verlag, 2008.

[6] G. N. Fursey, "Field emission and vacuum breakdown," *IEEE Trans. Elect. Insul.*, vol. EI-20, no. 4, pp. 659–670, Aug. 1985.

[7] E. E. Kunhardt, "Electrical breakdown of the space vacuum," *IEEE Trans. Plasma Sci.*, vol. 23, no. 6, pp. 970–979, Dec. 1995.

[8] G. H. Miley, *Direct Conversion of Nuclear Radiation Energy*. La Grange Park, IL: Amer. Nucl. Soc., 1970.

[9] V. Bobkov, "Studies of high voltage breakdown phenomena on ICRF antennas," Ph.D. thesis, Technische Universitat Munchen Fakultat Fur Physik, Garching, Germany, 2003.

[10] J. B. O. Caughman, C. Castano-Giraldo, M. Aghazarian, F. W. Baity, D. A. Rasmussen, and D. N. Ruzic, "Study of RF breakdown mechanisms relevant to an ICH antenna environment," in *Proc. 17th Top. Conf. Radio Freq. Power Plasmas*, 2007, p. 195.

[11] J. Knobloch, "Advanced thermometry studies of superconducting radio-frequency cavities," PhD thesis, Cornell Univ., New York, 1997.

[12] E. J. Grant, C. M. Posada, C. H. Castano, and H. K. Lee, "Electron field emission Particle in Cell (PIC) coupled with MCNPX simulation of a CNT-based flat-panel-X-ray source," in *Proc. SPIE Phys. Med. Imaging*, 2011, vol. 796108, pp. 1–11.

[13] C. H. Castano, "Unipolar Arcs," in *Proc. Workshop Unipolar Arcs*, Chicago, I L, Jan. 29, 2010.

[14] H. J. G. Gielen and D. C. Schram, "Unipolar arc model," *IEEE Trans. Plasma Sci.*, vol. 18, no. 1, pp. 127–133, Feb. 1990.

[15] N. Radic and B. Santic, "Floating potential and plasma sheath in vacuum arc plasma," *J. Appl. Phys.*, vol. 73, no. 11, pp. 7174–7179, Jun. 1993.

[16] J. D. Cobine, *Gaseous Conductors*. New York: Dover, 1941.

[17] R. L. Stoll, "Method of measuring alternating currents without disturbing the conducting circuit," *Proc. Inst. Elect. Eng.*, vol. 22, no. 10, pp. 1166–1167, Oct. 1975.

[18] J. D. Ramboz, "Machinable Rogowski coil design and calibration," *IEEE Trans. Instrum. Meas.*, vol. 45, no. 2, pp. 511–515, Apr. 1996.

[19] W. F. Ray and C. R. Hewson, "High performance Rogowski current transducers," in *Conf. Rec. 35th IEEE/IAS Annu. Meet. World Conf. Ind. Appl. Elect. Energy*, 2000, pp. 3083–3090.

[20] D. A. Ward, J. La, and T. Exon, "Using Rogowski coils for transient current measurements," *Eng. Sci. Educ. J.*, vol. 2, no. 3, pp. 105–113, Jun. 1993.

[21] Z. Insepov, J. Norem, and S. Veitzer, "Ion solid interaction and surface modification at RF breakdown in high-gradient linacs," in *Proc. 21st CAARI*, vol. 1336, *AIP conference proceedings*, Fort Worth, TX, Aug. 8–13, 2010, pp. 345–348.
[22] Z. Insepov, J. Norem, and S. Veitzer, "Atomistic self-sputtering mechanisms of RF breakdown in high-gradient linacs," *Nucl. Instrum. Methods Phys. Res. B, Beam Interact. Mater. At.*, vol. 268, no. 6, pp. 642–650, Mar. 2010. DOI:10.1016/j.nimb.2009.12.016.
[23] J. Norem, Z. Insepov, D. Huang, S. Mahalingam, and S. Veitzer, "The problem of RF gradient limits," in *Proc. 11th Int. Workshop Neutrino Factories Superbeams Beta Beams-NuFact09*, vol. 1222, *AIP conference proceedings*, 2010, pp. 348–352. DOI:10.1063/1.3399340.
[24] Z. Insepov, J. Norem, D. Huang, S. Mahalingam, and S. Veitzer, "Modeling RF breakdown arcs," in *Proc. PAC*, Vancouver, BC, Canada, May 4–8, 2009, pp. 800–802.
[25] Z. Insepov, J. Norem, T. Proslier, S. Mahalingam, and S. Veitzer, "Numerical modeling of arcs in accelerators," in *Proc. 25th LINAC*, Tsukuba, Japan, Sep. 12–17, 2010, pp. 205–207.
[26] Z. Insepov, J. Norem, S. Veitzer, and S. Mahalingam, "Modeling arcs," in *Proc. 19th Top. Conf. RF*, Newport, RI, Jun. 1–3, 2011, to be published.
[27] M. A. Lieberman and A. J. Lichtenberg, *Principles of Plasma Discharges and Materials Processing*. New York: Wiley-Intersci., 1994.
[28] C. H. Castaño G., "Study of breakdown/arcing for high power RF antennas on fusion applications," PhD thesis, Univ. Illinois, Champaign, IL, 2006.
[29] C. Gormezano, "Radio frequency heating and current drive—Status and prospects for the next step," *Fusion Eng. Des.*, vol. 14, no. 1/2, pp. 99–109, Apr. 1991.
[30] M. Tomitori, K. Sugata *et al.*, "Reproducibility of scanning tunneling spectroscopy of si(111) 7×7 using a build-up tip," *Surface Sci.*, vol. 355, no. 1–3, pp. 21–30, Jun. 1996.
[31] F. Schwirzke, "Unipolar arc model," *J. Nucl. Mater.*, vol. 128/129, pp. 609–612, Dec. 1984.
[32] N. K. Allen and R. V. Latham, "The energy spectra of high-β electron sites on broad-area copper electrodes," *J. Phys. D Appl. Phys.*, vol. 11, no. 4, pp. L55–L57, Mar. 1978.

Carlos H. Castano was born in Rionegro, Antioquia, Colombia, in 1973. He received the B.S. degree in chemical engineering from the National University of Colombia, Medellin, Colombia, in 1998 and the M.S. and Ph.D. degrees in nuclear engineering from the University of Illinois at Urbana-Champaign, Urbana, in 2002, and 2006, respectively.

He worked as a Postdoctoral Research Assistant in the Center for Plasma Materials Interaction in Urbana Illinois, in 2007. In 2008, he joined the Nuclear Engineering Department at Missouri University of Science and Technology (previously University of Missouri Rolla), Rolla. His current research interests include the development of vacuum insulation applications, radiation induced chemistry, and nuclear materials.

Dr. Castano is a Member of the American Nuclear Society, the Neutron Scattering Society of America, and the American Physical Society.

Maro Aghazarian is a global nomad, having visited seven countries in the last 3 years and lived in three different countries in her not-so-long lifetime. She also enjoys dancing tango, rock climbing, and volunteering to educate the public in her free time. She completed her B.S. in University of Illinois at Urbana-Champaign in 2005, before which she attended Los Angeles Pierce College for 2 years, where she started a mathematics club, and before that, finished high school in Tehran, where she was admitted to the Association of Young Mathematicians ranking 8/7000 and was the founder and editor of a school biweekly. She is now completing her Master's thesis on breakdowns in vacuum before she can move on to more adventures, which she'd love to include maximum learning.

John B. O. Caughman, II received the B.S. degree in electrical engineering from the University of South Carolina, Columbia, in 1984, and the M.S. and Ph.D. degrees in nuclear engineering from the University of Illinois at Urbana-Champaign, Urbana, in 1986 and 1989, respectively.

He worked as a Postdoctoral Researcher at the IBM T.J. Watson Research Center, Yorktown Heights, NY, from 1989 to 1991 and as a Staff Member for IBM, East Fishkill, NY, in 1991. In 1992, he joined the research staff at Oak Ridge National Laboratory, Oak Ridge, TN, and is currently a Senior Research Staff Member in the Fusion Energy Division. His current research interests include radio frequency breakdown, electron cyclotron and Bernstein wave heating, ion cyclotron antenna development, plasma diagnostics, and plasma-antenna-material interactions.

Dr. Caughman is a Member of the IEEE and the American Vacuum Society.

David N. Ruzic is the Director of the Center for Plasma Material Interactions at the University of Illinois. Having joined the faculty in 1984, he became a Professor in the Department of Nuclear, Plasma, and Radiological Engineering and became affiliated as well with the Department of Electrical and Computer Engineering and the Department of Physics. Since 2008, he has been an Assistant Professor of Nuclear Engineering in Missouri University of Science and Technology. His current research interests center on plasma processing for the microelectronics industry (deposition, etching, EUV lithography, and particle removal), atmospheric pressure plasmas for industrial applications, and on fusion energy research.

Dr. Ruzic is a Fellow of the American Nuclear Society and of the American Vacuum Society.